Available online at www.sciencedirect.com
ScienceDirect
Metabolism Clinical and Experimental 55 (2006) 1308–1316
Metabolism
Clinical and Experimental
www.elsevier.com/locate/metabol

Low-density lipoproteins generated during an oral fat load in mild hypertriglyceridemic and healthy subjects are smaller, denser, and have an increased low-density lipoprotein receptor binding affinity

Davide Noto, Manfredi Rizzo, Carlo Maria Barbagallo, Angelo Baldassare Cefalù, Alessia Lo Verde, Francesca Fayer, Alberto Notarbartolo, Maurizio Rocco Averna*

Department of Internal Medicine, University of Palermo, I-90127 Palermo, Italy

Received 8 February 2005; accepted 8 May 2006

Abstract

Triglyceride-rich lipoproteins generated during the postprandial phase are atherogenic. Large very low-density lipoproteins (LDLs) or chylomicrons (CMs) are not as atherogenic as their remnants (Rem). Small and dense LDLs are associated with cardiovascular disease. Low-density lipoprotein size is partly under genetic control and is considered as a relatively stable LDL feature. In this article, we present data on retinyl palmitate kinetics correlated with the modification of LDL features in terms of size, density, and in vitro receptor binding affinity after an oral fat load. Six nondiabetic, hypertriglyceridemic (HTG) patients and 6 healthy controls were examined. Low-density lipoprotein size was assessed by gradient gel electrophoresis, and LDL density by density gradient ultracentrifugation. Low-density lipoprotein binding affinity was tested by in vitro competition binding assay on normal human skin fibroblasts (HSFs) and hepatoma cells (HepG2). Kinetic parameters were estimated in CM and Rem fractions by compartmental modeling. Hypertriglyceridemic patients showed significantly higher triglyceride area and a slower CM fractional catabolic rate. Postprandial LDL density increased both in HTG patients and in the control group with a significant difference between groups at 6 hours. Fasting LDL size was lower in HTG patients vs controls but decreased similarly in the postprandial phase. Low-density lipoprotein size and density postprandial modifications were not correlated with any investigated parameter. Postprandial LDLs were internalized more efficiently by HSF than baseline LDL only in the HTG group. In conclusion, postprandial LDLs are smaller and denser compared with fasting LDLs after an oral fat load. Postprandial LDLs also slightly increased their affinity to the HSF cell receptors.

1. Introduction

Several studies have pointed out that the triglyceride (TG)-rich lipoproteins (TRLs) generated during the postprandial phase are atherogenic [1-3]. Large, very low-density lipoproteins (VLDLs) or chylomicrons (CMs) do not seem as atherogenic as their remnants (Rem) [4,5]. The measure of Rem generation during the postprandial phase is then a relevant issue and it has been extensively investigated [6]. Postprandial TG area has been widely used as an expression of postprandial TRL metabolism, but this measure shows poor sensitivity, TGs being present in large and small lipoprotein classes of both intestinal and hepatic origin [7]. Most of the TRLs are removed from circulation by apolipoprotein (apo) E–mediated uptake and the bulk of TGs reaching the liver is assembled in large VLDLs and dismissed into the circulation in the late postprandial phase [9]. Several authors have used retinyl palmitate (RP) during an oral fat load to label the lipoproteins of intestinal origin [8,9], and more than 75% of RP has been found associated with apoB48 between 4 and 6 hours after the feeding [9]. Abnormalities in the clearance rate of CM have been demonstrated in patients with type 2 diabetes mellitus [10,11] because visceral obesity and hyperinsulinism [12] of these patients strongly correlated with the degree of the metabolic impairment. Mild hypertriglyceridemia low HDL cholesterol phenotype has been linked to CM clearance impairment in nondiabetic subjects [13]. This atherogenic phenotype is also worsened by the presence of small and

* Corresponding author. Tel.: +39 91 6552936; fax: +39 91 6552936.
E-mail address: avernam@mbox.unipa.it (M.R. Averna).

0026-0495/$ – see front matter © 2006 Published by Elsevier Inc.
doi:10.1016/j.metabol.2006.05.015

dense LDLs. Low-density lipoprotein size is inversely correlated with the degree of impairment of the postprandial metabolism, measured by fasting and postprandial TG levels or RP clearance [13,14]. The size of LDL particles is influenced by metabolic factors such as the presence of large VLDLs in the plasma and/or the reduced free fatty acid trapping in the adipose tissue with free fatty acid hepatic overload [15]. Postprandial LDL size modifications after an oral glucose tolerance test have been reported [16], whereas some studies have shown LDL size and density variations after an oral fat load [17,18]. Alteration of LDL size and density during the postprandial phase may increase the role of LDL in determining the postprandial atherogenic profile. In this article we present data on the short-term changes of some atherogenic LDL features, such as size, density, and in vitro receptor binding activity, measured in nondiabetic hypertriglyceridemic (HTG) patients and healthy controls after an oral fat load. The modification of the LDL pattern in terms of size, density, and affinity for the receptor has been correlated with fasting and kinetic parameters after labeling intestinal TRLs and their Rems with RP. A simple compartmental model has been used to obtain kinetic measures.

2. Methods

2.1. Study subjects

Six HTG nondiabetic patients (age, 32 ± 4 years) and 6 healthy controls of comparable age, sex (5 men, 1 woman), and apoE genotype (all subjects were E3/E3) were enrolled in the Lipid Clinic of the Department of Internal Medicine of the University of Palermo (Palermo, Italy). All subjects were in hypolipidemic drug washout (at least 14 days); none of them had a history, symptoms, or clinical/instrumental diagnosis of coronary artery disease. Patients were selected on the basis of a known history of mild hypertriglyceridemia. The subjects were ruled out if their baseline TG value exceeded 400 mg/dL (4.5 mmol/L) before performing the experiment. Anthropometrical measurements were taken and a blood sample was used for genetic analyses and fasting lipid pattern determination.

2.2. Oral fat load protocol

After an overnight fasting, an oral fat load consisting of a mix of cheese, sugar, coffee, and milk was administered to the patients. The meal was balanced to give 77% lipids, 15% carbohydrates, and 8% protein by energy intake, and it contained vitamin A as RP. The meal was prepared to give 50 g fat and 50 000 vitamin A units per square meter of body surface. Thirty minutes before the meal and hourly until the 9th hour after the meal, blood was withdrawn in dim light; plasma was separated by centrifugation and immediately processed or stored at −80°C.

2.3. Lipid assay procedures

Plasma total cholesterol (TC), TG, and HDL cholesterol (HDL-C) levels after phosphotungstic acid precipitation were measured by using standard enzymatic-colorimetric procedures (Roche Diagnostics, Basel, Switzerland) on a COBAS MIRA plus autoanalyzer (Roche Diagnostics). Low-density lipoprotein cholesterol (LDL-C) was calculated by the Friedewald formula: LDL-C = TC − (TG/5) − HDL-C (values in milligrams per deciliter). In 1 patient with plasma TG level of 380 mg/dL, plasma LDL-C level was measured on the LDL fraction obtained by ultracentrifugation. The calculated LDL-C value was used in the data analysis because it did not differ significantly from the measured value. After calculations, all parameters were converted to millimoles per liter. Areas under the curve for TGs and RP were calculated by polygonal interpolation. Adjusted TG areas under the curve (minus baseline TG values) were also calculated. Triglyceride areas are expressed as milligram × hour/deciliter and RP areas as microgram × hour/liter.

2.4. Lipoprotein isolation

Fasting and postprandial lipoproteins were isolated by sequential ultracentrifugation [7]. The CM-containing fraction was obtained by overlying 4 mL of plasma with EDTA saline and centrifuging at 21 000 rpm for 40 minutes in an L90 K Optima Ultracentrifuge (Beckman Coulter, Fullerton, CA). The top CM-containing layer was washed with EDTA saline by an overnight centrifugation at 40 000 rpm to avoid residual plasma contamination. The infranatant from the first spin was overlaid with EDTA saline and spun at 40 000 rpm for 22 hours to obtain the Rem-containing fraction. The LDL and HDL fractions were obtained by sequentially increasing the density with potassium bromide in the range between 1.019-1.063 and 1.063-1.210 g/mL, respectively. All fractions were dialyzed against 10 mmol/L ammonium bicarbonate and frozen at −80°C.

2.5. Chylomicrons and Rem RP determination

Fasting and postprandial fractions containing CM and Rem were assayed. In some cases, aliquots of whole plasma and all fractions with density greater than 1.006 g/mL of the corresponding time point were also thawed to check for RP recovery. CM and Rem fractions accounted for almost all of the RP present in the plasma; in the other fractions, the amount detected was negligible (data not shown). Retinyl palmitate was measured by reverse-phase high-performance liquid chromatography (HPLC) using a method by Cortner et al [19] with some modifications. Briefly, the organic phases of CM and Rem fractions were extracted in ethanol-hexane-water (1:2:1). Ethanol contained retinyl acetate (20 μg/mL) as internal standard. Extracts were dried under nitrogen at 60°C, dissolved in 500 μL of methanol, and set in a 507 Gold Beckman HPLC autosampler (Beckman Coulter, Fullerton, CA). The HPLC run was performed on a Beckman ODS 2 C18 column (Beckman Coulter) at 50°C using a gradient of 10% to 30% tetrahydrofuran-water (9:1), starting after 5 minutes of 10% isocratic tetrahydrofuran-water (9:1) in methanol. Peaks

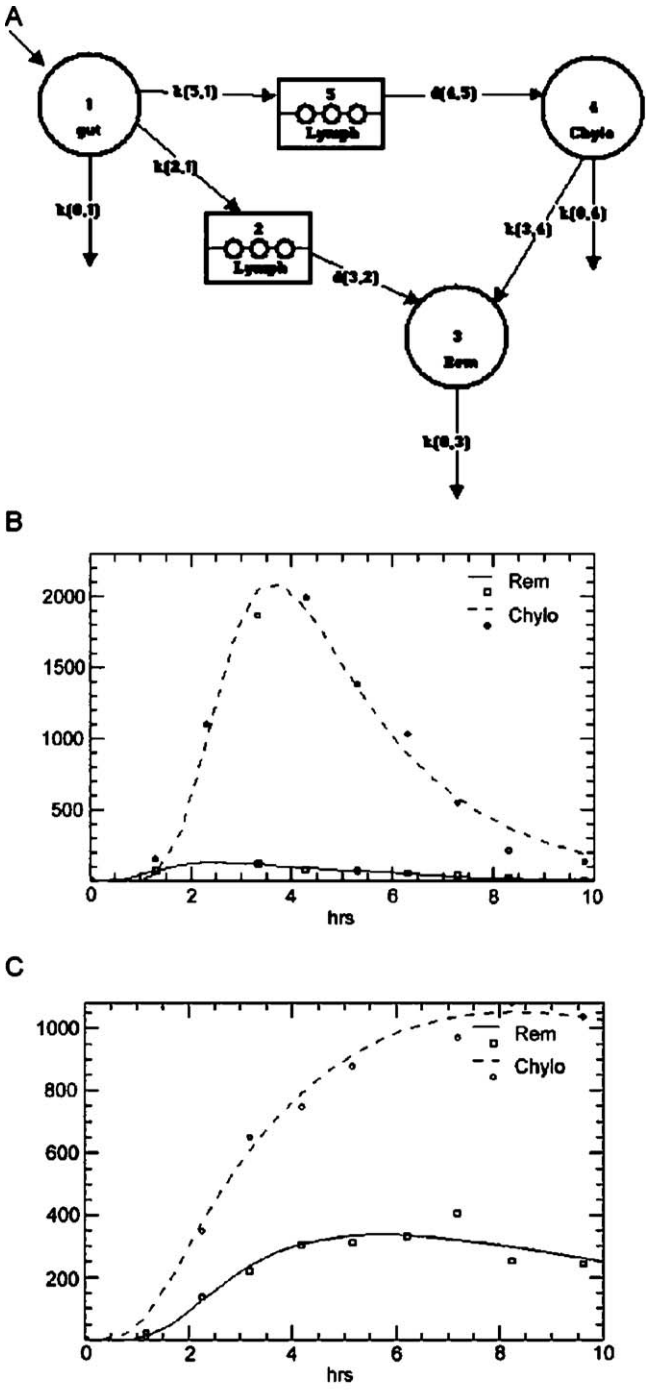

Fig. 1. Compartmental model of RP kinetics. A, Compartmental model. B and C, RP kinetics in CM (dashed line) and Rem fractions (solid line) in healthy control (B) and HTG subject (C).

were detected at 310 nm, identified, and calibrated against true standards of retinyl palmitate and retinyl acetate (Sigma, St. Louis, MO).

2.6. Low-density lipoprotein size

Low-density lipoprotein size was assessed by nondenaturing polyacrylamide gradient gel electrophoresis in 2% to 16% polyacrylamide commercial gels (Alamo Gels Co, San Antonio, TX) as described elsewhere [20]. Aliquots of LDL fractions of all subjects at baseline, 6 hours, and 9.5 hours were run into the gels and stained with Coomassie G250 stain afterward. Migration distances were used as references for calibration against samples of known LDL size (kindly provided by RM Krauss and PJ Blanche from the Lawrence Berkeley National Laboratory, Berkeley, CA), together with commercially available latex beads of different known diameters. Images of gels were digitally acquired with a DC120 Kodak (Eastman Kodak Company, Rochester, NY) digital camera and analyzed with the enclosed Kodak 1D-Science dedicated software. Calibration was performed by quadratic interpolation of the standard curve.

2.7. Low-density lipoprotein density gradient ultracentrifugation

Low-density lipoprotein subfractions obtained by preparative ultracentrifugation were divided into 4 discrete subclasses by using a previously described procedure for density gradient ultracentrifugation [21]. The LDL fractions were dialyzed for 24 to 48 hours against a sodium bromide solution (density [d] = 1.040 g/mL) at 4°C. The dialyzed fractions (3.5 mL) were then layered above a solution of d = 1.054 g/mL (4.5 mL) in a 12-mL Ultraclear Tube (Beckman Instruments, Palo Alto, CA) and 2.0 mL each of solutions of d = 1.024 and 1.019 g/mL were layered sequentially on the top. The tubes were centrifuged at 40 000 rpm for 44 hours at 15°C in a Beckman SW41 rotor. The contents of the tubes were then withdrawn sequentially in 5 discrete LDL

Table 1
Clinical data, lipids and kinetic parameters in HTG subjects vs controls

	Controls	HTG patients	P[a]
Clinical data, lipids			
Age (y)	28.5 ± 5.8	32.2 ± 3.8	ns
BMI (kg/m^2)	25.2 ± 4.8	26.2 ± 1.6	ns
Total cholesterol (mmol/L)	4.34 ± 1.2	5.83 ± 1.4	.05
TG (mmol/L)	0.95 ± 0.2	2.64 ± 1.4	.017
HDL-C (mmol/L)	1.02 ± 0.2	0.82 ± 0.1	ns
LDL-C (mmol/L)	2.88 ± 1.1	3.80 ± 1.0	ns
Total/HDL-C	4.6 ± 2.1	7.0 ± 1.1	.05
Oral fat load			
RP/CM ratio[b]	0.57 ± 0.47	0.16 ± 0.06	ns
RP/Rem ratio[b]	0.01 ± 0.01	0.14 ± 0.25	ns
CM FCR (pools/h)	2.9 ± 3.5	0.4 ± 0.5	.03
Rem FCR (pools/h)	1.8 ± 2.5	0.7 ± 0.5	ns
CM to Rem (pools/h)	0.05 ± 0.04	0.05 ± 0.03	ns
RP area CM (μg h/L)	4818 ± 2939	6278 ± 2177	ns
RP area Rem (μg h/L)	529 ± 323	844 ± 728	ns
TG area (mg h/dL)	1382 ± 837	3998 ± 1749	.03
TG area, baseline adjusted (mg hr/dL)	674 ± 466	1997 ± 1616	ns
TG peak (mmol/L)	5.7 ± 3.3	16.1 ± 6.7	ns
TG peak time (h)	4.39 ± 1.03	6.18 ± 2.4	ns
LDL parameters			
LDL density (%)[c]	0.27 ± 0.09	0.34 ± 0.06	ns
LDL size (nm)	27.0 ± 0.5	26.2 ± 0.7	.05

[a] Mann-Whitney test.
[b] Proportion of RP flowing to CM or Rem/total administered RP.
[c] Percent of LDL 3 + LDL 4 protein content/total LDL protein content.

subfractions: LDL-0 (2.5 mL, d = 1.017-1.022 g/mL), LDL-I (2.5 mL, d = 1.023-1.029 g/mL), LDL-II (2.5 mL, d = 1.030-1.040 g/mL), LDL-III (2.0 mL, d = 1.041-1.051 g/mL), LDL-IV (1.5 mL, d = 1.052-1.064 g/mL). The 1.0-mL bottom portion was discarded. Protein contents of the LDL total fraction and subfractions were measured by an automated BCA protein detection kit (Pierce Biotechnology, Rockford, IL) on a COBAS MIRA plus autoanalyzer (Roche Diagnostics). The resulting values were expressed as the ratio of the protein content of the denser fractions (LDL III and IV) and the total LDL protein content. Time of maximum LDL density peak in every individual was calculated by a second-order polynomial interpolation of the time curve of LDL density. Time of maximum LDL density was calculated at the maximum of the fitting polynomial function.

2.8. Low-density lipoprotein binding competition assay

Baseline and 6-hour LDL fractions of all subjects were tested in vitro for the receptor binding in competition assays against fluorescent di-octadecyl-indo-carbocyanine iodide (DIL)–labeled LDL. DIL LDLs were prepared as described elsewhere [22]. Human hepatoma cells (HepG2, 50 000/well) or human skin fibroblasts (75 000/well) were seeded onto 24-well plates (Corning Life Sciences, MA) and grown at 37°C, 5% CO_2, in Dulbecco modified Eagle's medium (DMEM glutamax, Gibco BRL, Gaithersburg, MD) supplemented with 10% fetal bovine serum, 100 U/mL penicillin, 100 μg/mL streptomycin (Gibco BRL), and 1% nonessential amino acids. Cells were grown to subconfluence. Forty-eight hours before the experiment, the medium was replaced with DMEM + 10% lipoprotein-depleted serum to overexpress the LDL receptor. The cells were washed twice with PBS and incubated for 4 hours at 37°C with 1 mL/well of DMEM + 10% lipoprotein-depleted serum + 20 μg/mL of DIL LDL alone or competed with 200 μg of the different cold LDL fractions. After 3 washes with cold PBS + 2 mmol/L $CaCl_2$ + 2 mmol/L $MgCl_2$, cells were lysed in 0.1 N NaOH and 0.1% sodium dodecyl sulfate (1% for HepG2 cells) at 37°C for 1 hour. Aliquots were used for protein commercial determinations (BCA micro, Pierce Biotechnology) and cell-incorporated fluorescence was read on an RXL10 fluorimeter equipped with a cell holder (Shimadzu Corporation, Tokyo, Japan) at 535 nm excitation and 570 nm emission. DIL LDL incorporation was calibrated against a DIL LDL scale in lysis buffer. Results were calculated as nanograms of incorporated DIL LDL per milligram of cell proteins and subsequently expressed as percent of DIL LDL displaced by a 10-fold molar excess of cold LDL at baseline or 6 hours after the administration of the fat load. All experiments were performed in triplicate.

2.9. Retinyl palmitate compartmental modeling

A minimal compartmental model was developed by using the SAAM II version 1.0 software (RFKA, Seattle, WA). The use of a minimal model has the advantage of simplifying calculations, reducing the number of differential equations to be solved in a unique solution by the system. This reduces the uncertainty in the estimation of kinetic data. Nevertheless, in 2 HTG subjects, the model was not able to describe accurately some secondary catabolic processes, generating unfitted shoulders on the main decay curves fitted by the model (see Fig. 1). Compartment 1 (Gut, 1) represents the intestine. RP load is introduced as a forcing function. In the attempt to mimic the absorption of fat by the intestine, different forcing functions were applied and the better way to describe the process was as a Gaussian curve with a delay (see Appendix A). After a further delay representing lipoprotein assembly and lymph transit (Lymph, 2,5), RP appeared both in the CM (Chylo, 4) and in the Rem (Rem, 3) plasma compartments. The direct appearance of RP in the Rem fraction is a compartmental definition; it does not necessarily imply direct Rem generation by the intestine. The model does not aim to explain the underlying biochemical mechanism. Once in the plasma, CM RP is either removed [k(0,4)] or converted into Rem RP [k(3,4)]. Remnant RP can only be removed [k(0,3)]. All estimated kinetic parameters and equations are shown in Appendix A.

2.10. Statistics

Differences in the investigated parameters among the study groups were assessed parametrically by t test for independent data, and nonparametrically by the Mann-Whitney

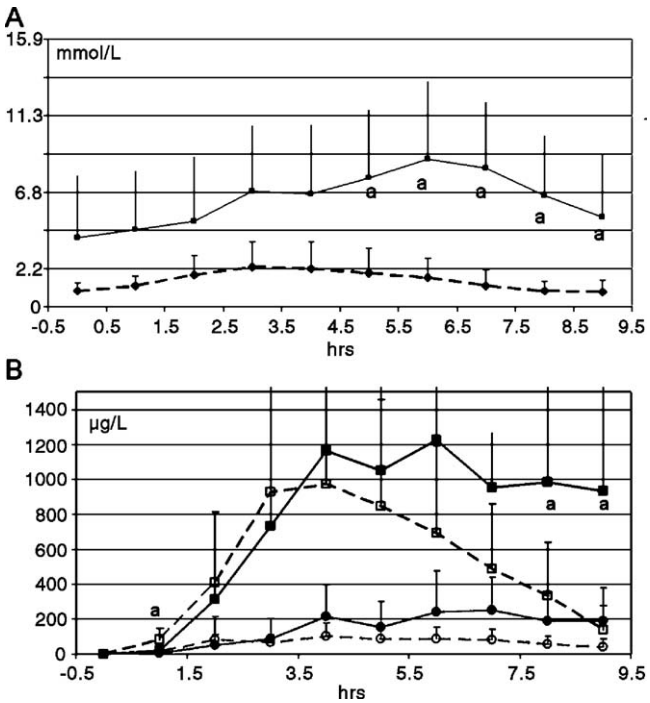

Fig. 2. Postprandial plasma curves of TGs and RP. A, Triglyceride plasma levels in HTG subjects (solid line) vs controls (dashed line). B, Retinyl palmitate in CM (squares) and Rem (circles) fractions in HTG patients (solid line, filled points) vs controls (dashed line, empty points). $^{a}P < .05$, HTG patients vs controls; t test.

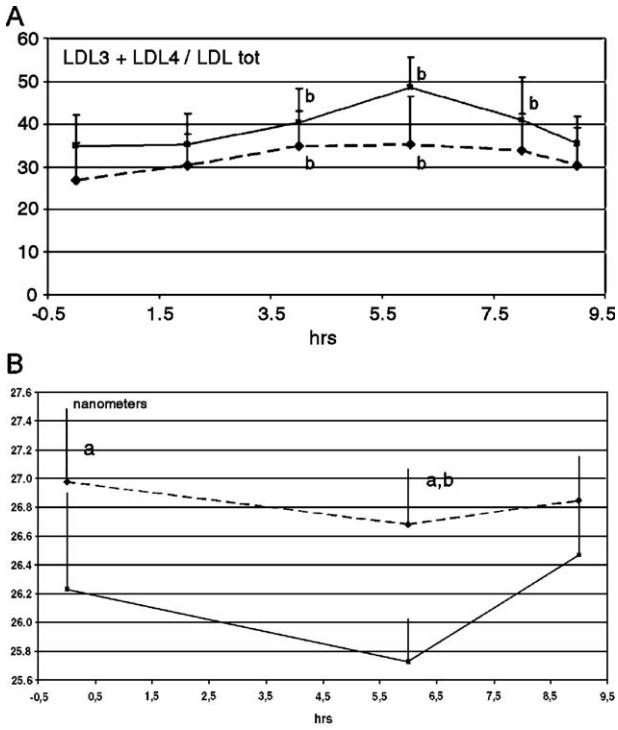

Fig. 3. Postprandial plasma variation in LDL size and density. A, LDL density (LDL 3-4/LDL total; see text). B, LDL size (angstrom) in HTG subjects (solid line) vs controls (dotted line). [a]$P < .05$, HTG patients vs controls; t test. [b]$P < .05$, time points vs baseline; t test.

test. Univariate correlation was assessed by calculating Spearman rank-order correlation coefficients. Analyses were sex adjusted by using a sex numeric variable. Fasting and postprandial LDL affinity for the receptors were evaluated by t test for paired data using triplicate observations for each individual. All statistics were performed by using the Crunch 4.0 statistical package (Crunch Software Corporation, Oakland, CA).

3. Results

3.1. Baseline and kinetic parameters

Differences in clinical data, lipids, kinetic parameters, and LDL features are shown in Table 1. Hypertriglyceridemic patients had significantly higher TC and TGs. Postprandial TG area was significantly greater in HTG patients vs controls, but the areas were not significantly different after correction for baseline TG levels (average postprandial TG levels ± SD are presented in Fig. 2A). Sixteen percent of RP in HTG patients vs 57% in controls entered the circulation (P = nonsignificant [ns]). Chylomicron fractional catabolic rate (FCR) and Rem FCR were, respectively, 7-fold ($P = .03$) and 2.5-fold higher (P = ns) in controls than in HTG patients. Direct Rem entrance in the plasma was 14-fold (P = ns) higher in HTG patients; the conversion rate between CM and Rem was similar between the 2 groups.

Retinyl palmitate curves are shown in Fig. 2B. Data are graphed as mean ± SD. RP maximum peak was delayed and RP clearance was impaired in HTG patients (RP levels at 8 and 9 hours significantly differed from controls; t test, $P < .05$).

Table 2
Nonparametric Spearman correlation of LDL postprandial parameters with lipid parameters

	LDLD0	LDLD6	LDLDΔ	LDLS0	LDLS6	LDLSΔ
HTG	0.45	0.59	0.38	−0.44	**−0.87**	0.25
P	ns	ns	ns	ns	**0.002**	ns
LDL-C	0.48	**0.73**	0.16	−0.34	−0.54	0.06
P	ns	**0.01**	ns	ns	ns	ns
TG area	0.21	0.61	0.58	−0.24	−0.37	−0.17
P	ns	ns	ns	ns	ns	ns
TG peak	0.45	**0.75**	0.46	−0.4	−0.62	−0.11
P	ns	**0.01**	ns	ns	ns	ns

Significant tests in bold. Nonsignificant correlation with other parameters are not shown. LDLD indicates LDL density; LDLD0, baseline levels; LDLD6, 6 hours; LDLDΔ, individual variation between baseline and 6 hours; LDLS, LDL size; HTG, hypertriglyceridemia (yes/no); TG area, postprandial plasma TG area; TG peak, maximum postprandial plasma TG value.

3.2. Postprandial LDL size and density modifications

The postprandial increase of LDL density is shown in Fig. 3A as the ratio between LDL III + LDL IV protein content by total LDL protein content (mean ± SD). The LDL density ratio in HTG patients was not significantly higher at baseline compared with controls, but LDL density increased with a maximum at 6 hours in both groups (HTG patients vs controls; t test, $P < .05$) and decreased in the late hours of the study. Low-density lipoprotein size change was inversely correlated with the LDL density postprandial increase. Low-density lipoprotein size also decreased after 6 hours in both the control and HTG groups with a slight increase at the end of the study. The HTG group also showed lower fasting LDL size (Table 1, Fig. 3B).

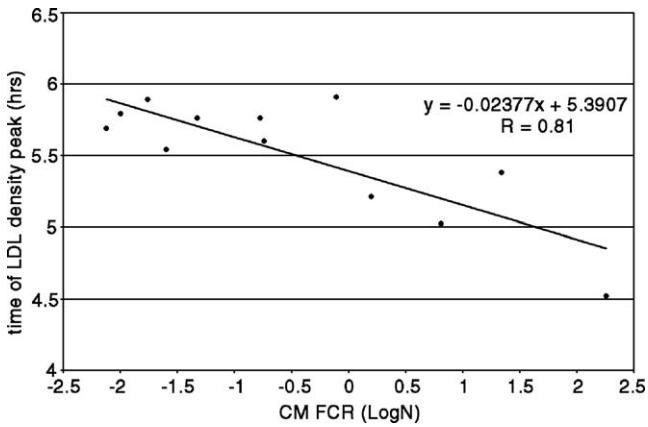

Fig. 4. Chronological correlation of CM clearance rate with postprandial LDL density increase. Chylomicron clearance rate is expressed in the abscissa as logarithm of CM FCR. Postprandial LDL density increase over time is expressed in the ordinate as the time when the maximum LDL density increase was reached (see Methods). Shown is the equation of the regression line with the corresponding Pearson P.

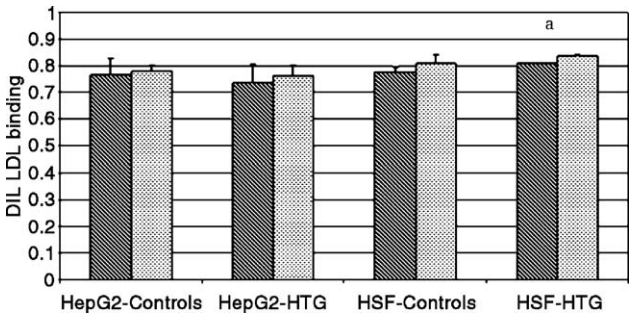

Fig. 5. Fluorescent LDL displacement by a 10-fold excess of patients' LDLs at baseline and at 6 hours. HSF indicates human skin fibroblasts. Controls vs HTG subjects; percent displacement by baseline LDL (dashed bars) and by 6-hour LDL (dotted bars). $^{a}P < .05$, t test for paired data; baseline LDL vs postprandial LDL. Plotted on the y-axis is the ratio of DIL LDL binding with cold LDL competitors and without cold LDL competitors.

3.3. Correlation of TRL metabolism with postprandial LDL modifications

The associations between fasting/fed LDL features and the investigated parameters were tested with the Spearman rank-order correlation (Table 2). Fasting LDL density (LDLD 0) and individual LDL density Δ variation between baseline and 6 hours (LDLD D) were not associated with any parameter, whereas LDL density at 6 hours (LDLD 6) was correlated with LDL-C levels and TG maximum postprandial peak. Fasting LDL size (LDLS 0) was not correlated with any parameter, whereas LDL size at 6 hours (LDLS 6) was correlated negatively with the HTG status. The individual LDL size Δ variation between baseline and 6 hours (LDLS D) was not correlated with any parameter.

The chronological relationship between CM clearance and LDL size is outlined in Fig. 4. This Cartesian chart shows that CM clearance (expressed by logarithm of CM FCR in the x-axis) is inversely correlated with the time of maximum LDL density (Pearson $R = 0.81$; $P = .006$), indicating that subjects with faster CM clearance show earlier modifications of postprandial LDL density.

3.4. Postprandial LDL affinity to the cell receptor

Results of the in vitro competition assays are described in Fig. 5. Both in liver HepG2 cells and in human skin fibroblasts, postprandial LDLs at 6 hours were more able to displace fluorescent LDLs from cell internalization than baseline LDLs (experiments in triplicate). Postprandial LDLs gained about 2% to 3% of displacement. The gain in binding affinity was significant only in the fibroblast model and for the HTG subjects, but the trend was similar in both study groups.

4. Discussion

Atherogenicity of postprandial lipemia has been widely investigated [23]. Although postprandial lipoproteins are too large to be internalized in the arterial wall, they are trapped by surface proteoglycans and delipidated by lipoprotein lipase and endothelial lipase, generating smaller lipoprotein Rem that enter the arterial wall. In addition, lipoprotein oxidation can contribute to postprandial lipoprotein atherogenicity. Side products of lipolysis, such as lysolecithin, have been shown to induce the expression of different atherogenic genes, including adhesion molecules, impairing the production of nitric oxide [23]. Several studies have pointed out the role of different factors affecting postprandial lipemia; age, obesity, smoking habit, apoE genotype, fatty acid binding protein 2, and lipoprotein lipase polymorphisms are only some of the factors playing a role in TRLs catabolism.

Small and dense LDLs are associated with cardiovascular disease. Prospective studies have shown that small LDL particles are associated with a more than 3-fold increase in cardiovascular risk [24].

In the Québec Cardiovascular Study, multivariate and subgroup analyses showed that small, dense LDL particles are predictive of cardiovascular disease independently of LDL-C, TG, HDL-C, and apoB levels and the TC/HDL-C ratio [25].

4.1. Oral fat load and compartmental modeling

The administration of a standardized oral fat meal is one of the most common procedures to investigate postprandial metabolism. Such procedure is used worldwide and represents a lipid overload able to stress the postprandial lipid metabolism. Simultaneous administration of RP with the fat meal has increased the amount of information obtained by the fat load alone. Retinyl palmitate administered with the meal labels the lipoproteins of intestinal origin, tracing irreversibly their catabolic fate. Kinetic data of RP clearance have been analyzed by compartmental modeling [26,27], although its validity is still under discussion [28]. One of the main limitations in the kinetic modeling of the TRL metabolism is that it does not represent an "ideal" system in steady-state equilibrium. The fat load induces complex perturbation in the system, so that clearance rates are not stable over time but change as a function of the amount of TRLs to be cleared [29]. Consequently, studies dealing with postprandial metabolism and the estimation of TRL FCRs showed controversial results [28-30]. In this article, a minimal compartmental model has been used. This model is an extreme simplification of previous models that used many compartments to exactly fit the RP curves. The use of a minimal model decreased the uncertainty in the estimated solutions and resulting in low standard deviations associated to the parameters. However, the model was only able to fit the clearance curves by using first-order exponential decays. Small deviations from the main curves could be taken into account by more complex models, but in the current context, with large difference in clearance rates between HTG patients and controls, the use of a more complex model would give only a slight improvement. Even with these limitations, our estimates closely resemble previous results

obtained with intravenous administration of radiolabeled TRLs, showing FCRs in the range of 2 pools per hour [29]. Our data show that CM FCR was, as expected, about 7-fold slower in HTG patients than in controls, whereas Rem FCR was only 2-fold slower in HTG patients (not significant). More RP was found in the Rem fraction of the HTG patients during the study; TG area and maximum peak were also higher in the same study group. In some HTG subjects, RP was transferred directly from the intestine to the plasma Rem compartment. This path of RP flowing to Rem was not present in the control group model. The underlying mechanism explaining the appearance of RP directly in the Rem compartment is not clear. In these patients, enterocytes may produce denser lipoproteins in the range of VLDLs, corresponding to the Rem density range, or larger TRLs may be rearranged to smaller lipoproteins during the lymph transit. Our model is not able to test these hypotheses.

4.2. Low-density lipoprotein size and density in postprandial phase

Most of the studies that performed an oral fat load have shown that LDL-C levels are slightly increased or unchanged in the postprandial phase, whereas even less is known about modifications of LDL qualitative features, such as LDL size or density. Low-density lipoprotein size is considered a relatively stable feature of an LDL particle, related to the extent of lipolysis of large VLDL1 through TG exchange and subsequent hydrolysis [15]. In an early report, a postprandial increase of the mean LDL size due to an LDL III subfraction decrease was found in patients with type 2 diabetes mellitus and in controls [17]. This finding was not confirmed in a more recent study showing an opposite trend of the LDL changes with a decrease of LDL size in late postprandial phase [18]. In a recent report, even an oral glucose tolerance test was able to induce a small LDL size decrease [16]. In the present study, we evaluated the change in LDL features, such as size, density, and receptor affinity, in nondiabetic, mildly HTG young patients and healthy controls. Low-density lipoprotein density first, and then LDL size, were analyzed during the postprandial phase. Low-density lipoprotein density increased gradually with a peak at 6 hours (Fig. 3A), about 2 hours later than the CM palmitate peak. This was observed in HTG patients and controls. Low-density lipoprotein size decreased similarly in both groups (Fig. 3B). As mentioned earlier, these findings confirm the results of a recent study that demonstrated a decrease in postprandial LDL size in 49 overweight patients after an oral fat load [18]. Our article extends this observation, showing, in addition to the postprandial LDL size decrease, a parallel increase of postprandial LDL density and a modification of receptor binding affinity. In these studies, the average LDL size variation was small (about 0.2 nm), whereas in our study the decrease of LDL size was 0.5 nm in HTG patients and 0.3 nm in controls during the oral fat load. Probably the fat load represented a more intense stress for the postprandial lipolysis/clearance mechanism than the oral glucose tolerance performed in one of the studies; on the other hand, the impaired TRL catabolism of our selected HTG patients may lead to a bigger impact on the postprandial generation of smaller and denser LDLs compared with studies that performed an oral fat load in other types of patients. Using a nonparametric Spearman correlation test, no parameters were able to describe the individual LDL size and density variation between baseline and 6 hours of the oral fat load.

We also found a chronological correlation between the efficiency of the RP clearance and the appearance of small and dense LDLs in the plasma. As shown in Fig. 4, subjects with faster CM catabolism, identified by faster CM clearance rate (expressed as logarithm of CM FCR), showed an earlier increase in plasma LDL density (expressed as the time of the maximum LDL density increase); on the other hand, subjects with slower TRLs catabolism (low CM clearance rate) showed a delayed LDL density increase. Although these data were obtained in few subjects the correlation is statistically significant (Pearson correlation $P = .006$); this finding suggests that postprandial LDL size and density variation may partly depend on the efficiency of the lipolytic mechanism. In fact, the theory of generation of small LDLs by lipolysis of large VLDLs is not supported by clear kinetic evidence [31].

4.3. Postprandial vs fasting LDL affinity for the cell receptor

Baseline and postprandial (6 hours) LDLs were also tested for modifications of LDL receptor binding affinity in vitro using human fibroblasts and hepatoma HepG2 cells. Low-density lipoprotein at 6 hours from both HTG and control subjects showed more binding affinity than baseline LDL in both cell models. Nevertheless, the increase in binding affinity was very small, between 2% and 3% of DIL LDL displacement by a 10-fold molar excess of patients' LDLs, and the difference was significant only for HTG subjects in the fibroblast model. This finding may suggest that smaller postprandial LDLs are internalized slightly more efficiently by the LDL receptor. We correlated the increase in postprandial LDL binding with the modifications of LDL size. At least 50% of the increase of the affinity for the cell receptor is explained by the decrease in postprandial LDL size in the fibroblast model (Pearson $R = -0.584$, $P < .005$; data not shown). This finding explains why only in HTG patients, showing the greatest difference between fasting and postprandial LDL size, we could find a significant increase in the LDL affinity to the receptors. In contrast with this finding, previous studies showed that in fasting status, smaller LDLs bind the receptor with lower affinity [32]. Modifications of the LDL apolipoprotein content should be taken into account to explain how small LDLs seem to bind the receptor with higher affinity only in the postprandial phase. Postprandial LDLs are quite different from fasting LDLs. Postprandial lipoproteins are enriched in apoCIII and apoE that are known to interfere with the apoB100 binding

to the LDL receptor [33]. The postprandial LDL internalization may also be facilitated by modifications of the cell surface proteoglycan matrix. An increased affinity to proteoglycans may represent an atherogenic mechanism, considering that smaller particles are known to cross easily the arterial wall with the previously mentioned mechanism involving proteoglycan trapping, delipidation by lipases, and internalization [23]. Further studies are required to properly address the issues raised by these findings.

In conclusion, after an oral fat load, postprandial LDLs are smaller and denser. Postprandial LDLs show a slight increase in the affinity for cell surface receptors, but a significant increase was found only in the HTG subjects and in the fibroblast cell model.

Appendix A. Compartmental model equations and explanations

CM FCR = k(0,4) + k(3,4); fraction of CM plasma pool cleared in 1 time unit

Rem FCR = k(0,3); fraction of Rem plasma pool cleared in 1 time unit

CM to Rem = k(3,4)/CM FCR; fraction of CM removed from plasma by conversion to Rem

RP to CM = k(5,1)/(k(2,1) + k(5,1) + k(0,1)); fraction of RP transferred from gut to the CM plasma compartment.

RP to Rem = k(2,1)/(k(2,1) + k(5,1) + k(0,1)); fraction of RP transferred from gut to the Rem plasma compartment

RP out = k(0,1)/(k(2,1) + k(5,1)+k(0,1)); fraction of unabsorbed RP

Forcing function: ex1 = (vitamin A amount)/(SA × 2.51)exp(−((t−MA)^2)/(2 × SA^2)) (where vitamin A amount is expressed in micrograms after conversion from vitamin A units, SA is the width of the Gaussian curve, and MA is the time of maximum vitamin A peak in the intestine.

References

[1] Karpe F. Postprandial lipoprotein metabolism and atherosclerosis. J Intern Med 1999;246:341-55.

[2] Simpson HS, Williamson CM, Olivecrona T, Pringle S, Maclean J, Lorimer AR, et al. Postprandial lipemia, fenofibrate and coronary artery disease. Atherosclerosis 1990;85:193-202.

[3] Patsch JR, Miesenbock G, Hopferwieser T, et al. Relation of triglyceride metabolism and coronary artery disease: studies in the postprandial state. Arterioscler Thromb 1992;12:1336-45.

[4] Schaefer EJ, Gregg RE, Ghiselli G, Forte TM, Ordovas JM. Familial apolipoprotein E deficiency. J Clin Invest 1986;78:1206-19.

[5] Havel R. Triglyceride-rich lipoproteins and atherosclerosis—new perspectives. Am J Clin Nutr 1994;59:795-9.

[6] Ooi TC, Cousins M, Ooi DS, Steiner G, Uffelman KD, Nakajima K, et al. Postprandial remnant-like lipoproteins in hypertriglyceridemia. J Clin Endocrinol Metab 2001;86:3134-42.

[7] Ruotolo G, Zhang H, Bentrianov V, Le NA. Protocol for the study of the metabolism of retinyl esters in plasma lipoproteins during postprandial lipemia. J Lipid Res 1992;33:1541-9.

[8] Krasinski SD, Cohn JS, Russell RM, Schaefer EJ. Postprandial plasma vitamin A metabolism in humans: a reassessment of the use of plasma retinyl esters as markers for intestinally derived chylomicrons and their remnants. Metabolism 1990;39:357-65.

[9] Cohn JS, Johnson EJ, Cohm SD, Milne RW, Marcel JL, Russel RM, et al. Contribution of apoB48 and apoB100 triglyceride rich lipoprotein (TRL) to postprandial increases in the plasma concentrations of TRL triglycerides and retinyl esters. J Lipid Res 1993; 34:2023.

[10] Mero N, Syvanne M, Eliasson B, Smith U, Taskinen MR. Postprandial elevation of ApoB-48–containing triglyceride-rich particles and retinyl esters in normolipemic males who smoke. Arterioscler Thromb Vasc Biol 1997;17:2096-102.

[11] Tan KC, Cooper MB, Ling KL, Griffin BA, Freeman DJ, Packard CJ, et al. Fasting and postprandial determinants for the occurrence of small dense LDL species in non–insulin-dependent diabetic patients with and without hypertriglyceridaemia: the involvement of insulin, insulin precursor species and insulin resistance. Atherosclerosis 1995; 113:273-87.

[12] Taira K, Hikita M, Kobayashi J, Bujo H, Takahashi K, Murano S, et al. Delayed post-prandial lipid metabolism in subjects with intra-abdominal visceral fat accumulation. Eur J Clin Invest 1999;29: 301-8.

[13] Lemieux I, Couillard C, Pascot A, et al. The small, dense LDL phenotype as a correlate of postprandial lipemia in men. Atherosclerosis 2000;153:423-32.

[14] Katzel LI, Krauss RM, Goldberg AP. Relations of plasma TG and HDL-C concentrations to body composition and plasma insulin levels are altered in men with small LDL particles. Arterioscler Thromb 1994;14:1121-8.

[15] Kwiterowich PO. Clinical relevance of the biochemical, metabolic, and genetic factors that influence low-density lipoprotein heterogeneity. Am J Cardiol 2002;90:30i-47i.

[16] Okumura K, Matsui H, Kawakami K, Morishima I, Numaguchi Y, Murase K, et al. Modulation of LDL particle size after an oral glucose load is associated with insulin levels. Clin Chim Acta 1998; 276:143-55.

[17] Attia N, Durlach V, Paul JL, Soni T, Betoulle D, Girard-Globa A. Modulation of low density lipoprotein subclasses by alimentary lipemia in control and normotriglyceridemic non–insulin-dependent diabetic subjects. Atherosclerosis 1995;113:197-209.

[18] Blackburn P, Cote M, Lamarche B, Couillard C, Pascot A, Tremblay A, et al. Impact of postprandial variation in triglyceridemia on low-density lipoprotein particle size. Metabolism 2003;52:1379-86.

[19] Cortner JA, Coates PM, Le NA, Cryer DR, Ragni MC, Faulkner A, et al. Kinetics of chylomicron remnant clearance in normal and in hyperlipoproteinemic subjects. J Lipid Res 1987;28:195-206.

[20] Rizzo M, Barbagallo CM, Severino M, Polizzi F, Onorato F, Noto D, et al. Low-density-lipoprotein peak particle size in a Mediterranean population. Eur J Clin Invest 2003;33:126-33.

[21] Chapman JM, Laplaud MP, Luc G, et al. Further resolution of the low-density lipoprotein spectrum in normal human plasma: physicochemical characteristics of discrete subspecies separated by density gradient ultracentrifugation. J Lipid Res 1988;29:442-58.

[22] Corsetti JP, Weidner CH, Cianci J, Sparks CE. The labeling of lipoproteins for studies of cellular binding with a fluorescent lipophilic dye. Anal Biochem 1991;195:122-8.

[23] Goldberg IJ, Kako Y, Lutz EP. Responses to eating: lipoproteins, lipolytic products and atherosclerosis. Curr Opin Lipidol 2000; 11:235-41.

[24] Carmena R, Duriez P, Fruchart JC. Atherogenic lipoprotein particles in atherosclerosis. Circulation 2004;109(23 Suppl 1):III2-III7.

[25] Lamarche B, St-Pierre AC, Ruel IL, Cantin B, Dagenais GR, Despres JP. A prospective, population-based study of low density lipoprotein particle size as a risk factor for ischemic heart disease in men. Can J Cardiol 2001;17:859-65.

[26] von Reinersdorff D, Green MH, Green JB. Development of a compartmental model describing the dynamics of vitamin A metabolism in men. Adv Exp Med Biol 1998;445:207-23.

[27] Le NA, Coates PM, Gallagher PR, Cortner JA. Kinetics of retinyl esters during postprandial lipemia in man: a compartmental model. Metabolism 1997;46:584-94.

[28] Redgrave TG, Watts GF, Martins IJ, Barrett PH, Mamo JC, Dimmitt SB, et al. Chylomicron remnant metabolism in familial dyslipidemias studied with a remnant-like emulsion breath test. J Lipid Res 2001; 42:710-5.

[29] Berr F. Characterization of chylomicron remnant clearance by retinyl palmitate label in normal humans. J Lipid Res 1992;33:915-30.

[30] Park Y, Damron BD, Miles JM, Harris WS. Measurement of human chylomicron triglyceride clearance with a labeled commercial lipid emulsion. Lipids 2001;36:115-20.

[31] Berneis KK, Krauss RM. Metabolic origins and clinical significance of LDL heterogeneity. J Lipid Res 2002;43:1363-79.

[32] Chappell DA, Fry GL, Waknitz MA, Berns JJ. Ligand size as a determinant for catabolism by the low density lipoprotein (LDL) receptor pathway. A lattice model for LDL binding. J Biol Chem 1991;266:19296-302.

[33] Dallongeville J, Bauge E, Lebel P, Fruchart JC. Fat ingestion is associated with increased levels of apoC-III– and apoE-B–containing lipoprotein particles in humans. Eur J Clin Invest 1997;27: 1055-60.